Indian Journal of Pure & Applied Physics
Vol.54, May 2016, pp. 307-312

Structural and optical study of yttrium oxide co-doped with bismuth and zinc prepared by sol-gel method

G Bhavani[1]* & S Ganesan[2]

[1]Department of Physics, Jansons Institute of Technology, Karumathampatti Coimbatore 641 659, India
[2]Sri Shakthi Institute of Engineering and Technology, Coimbatore 641 062, India

Received 17 July 2015; revised 15 December 2015; accepted 11 January 2016

Bismuth and zinc co-doped Y_2O_3 samples are synthesized by sol-gel method using ammonium hydroxide as a precipitating agent. Structural analysis is done by XRD, SEM- EDAX and the optical properties are analysed by FTIR, UV-Vis absorption studies and photoluminescence (PL) studies. UV-Vis absorption studies show absorption only around 340 nm whereas PL shows peaks around 401 nm, 680 nm and 1020 nm forY_2O_3 co-doped with bismuth and zinc. The PL spectrum shows emission in violet region (401 nm) due to zinc dopant and red and NIR region (680 nm and 1020 nm) due to the bismuth dopant. This is a new material which can effectively work as an efficient and cheap red phosphor.

Keywords: Phosphoresence, Photoluminescence, Sol-gel, FTIR, XRD

1 Introduction

Nanocrystalline powders due to their average particle size (below 100 nm) may show different behaviours resulting from a higher surface energy due to the large surface area and the wider gap between the valence band and conduction band. The optimization of an efficient phosphor requires proper selection of the host and the activator material. The activators should be red, green and blue line emitters preferably with localized transition leading to efficient trapping center for high efficiency. The rare-earth (RE) activators satisfy the above requirements with the exception that the excited carriers in the host transfer rather slowly to the rare-earth activators. Yttrium oxide is the most familiar yttrium compound, which is popularly known as host for ion doping of other rare earth elements.Y_2O_3 activated by another group of important activators, like zinc and the so-called mercury-like ions, of which Bi3+ is one, are poorly studied[1,2]. Such compounds can be used as scintillators in luminescent screens or mercury-free luminescent photomultiplier bulbs. The spectral properties of these materials have been well studied[1-4]. Therefore, the investigation of Y_2O_3 is timely and addressed herein.

Y_2O_3: Eu, Bi red phosphors were prepared by homogeneous co-precipitation by Chi *et al.*[5] Eu^{3+} and Tb^{3+} doped Y_2O_3 nanoparticles have been synthesized by hydrothermal process by Singh *et al.*[6] Y_2O_3:Yb^{3+}–Er^{3+} were prepared by using Na_2S at a lower cost than that of other sulfuration processes by Lopez-Luke *et al.*[7] Er^{3+}-Yb^{3+} and Eu^{3+}-Er^{3+}-Yb^{3+} co-doped Y_2O_3 phosphors were synthesized at low temperature. Urea assisted combustion technique due to near infrared (NIR) diode laser excitation have been performed by Dey *et al.*[8] Back *et al.*[9] synthesized Bi- and Er-codoped Y_2O_3 nanocrystals by means of Pechini type sol-gel process. Y_2O_3:Eu^{3+} phosphors codoped with Yb^{3+} were synthesized by combustion synthesis process by Pandey *et al.*[10] Eu, Tb-codoped Y_2O_3 nanophosphors were synthesized by the combustion synthesis method by Som and Sharma[11]. Tm^{3+}/Er^{3+}/Yb^{3+} co-doped Y_2O_3–ZnO nano-composite was synthesized using the solution combustion technique by Yadav *et al.*[12] Er^{3+}/Yb^{3+} co-doped Y_2O_3 phosphors obtained by solution combustion reaction by Singh *et al.*[13] Y_2O_3: Eu^{3+},Sm^{3+}, Dy^{3+} phosphor were synthesized via solid state reaction method by Suresh *et al.*[14] Zn co-doped Y_2O_3 -Eu, Er and Tm prepared by sol-gel method were studied by Kottaisamy and Nakanishi[15]. Europium and lithium codoped yttrium oxide samples in which lithium concentration varied was done by Stanton *et al.*[16] Fine yttrium oxide powders doped with Yb^{3+} and co-doped either with Tm^{3+} or Ho^{3+} were synthesized via spray pyrolysis by Lojpur *et al.*[17] Tm^{3+}/Yb^{3+} co-doped Y_2O_3 nanophosphor has been synthesized by the solution combustion technique by Mishra *et al.*[18] It is observed from the literature survey of co-doped yttrium oxide

*Corresponding author (E-mail: bhavaneeg@gmail.com)

samples that co-doping increases the efficiency of the yttrium oxide based materials for applications. However, Zn^{2+} and Bi^{3+} combination of co-doping with yttrium oxide as a host by simple precipitation technique and with different but equal dopant concentration is rarely studied. Hence, an attempt has been made to synthesize bismuth and zinc co-doped yttrium oxide samples by simple precipitation techniques sol-gel method by using ammonium hydroxide as precipitating agents with three different dopant concentration and analyse their structural and optical properties.

2 Experimental details

2.1 Sol-gel method

To prepare pure sample, A Pure, 1 g of yttrium nitrate hexahydrate ($Y(NO_3)_3.6H_2O$) was dissolved in 10 mL of distilled water and stirred for long time to dissolve the salt completely, followed by ammonium hydroxide, the precipitating agent, added in drops to get a clear solution. Continuous stirring lead to precipitation and the precipitate was left for 15 h to settle. Then the obtained precipitate was washed with water and dried in an oven at 373 K for 3 h. After drying, the powder was finely ground. Calcination was done by heating the sample at 623 K in a muffle furnace for 15 h to obtain pure yttrium oxide[19].

To prepare doped yttrium oxide powders, ABZ1, ABZ2 and ABZ3, 1 g of Yttrium nitrate hexahydrate was dissolved in 10 mL of distilled water and stirred for long time to dissolve the salt completely. Then dopant precursor of 0.25, 0.5 and 1 weight percentage of yttrium precursor of equal dopant concentration respectively were added to the solution followed by the addition of 50 ml of ammonium hydroxide. Continuous stirring lead to precipitation and the precipitate was left for 15 hours to settle. Then the obtained precipitate was washed with water and dried in an oven at 373 K for 3 hours. After drying, the powder was finely ground. Calcination is done by heating the sample at 623 K in a muffle furnace for 15 hours to obtain doped yttrium oxide powder[19].

2.2 Characterisation

The powder XRD study was carried out using a Shimadzu XRD 6000 X-ray diffractometer using CuKα radiation. The morphological investigation of the samples was performed in JEOL Model JSM - 6390LV scanning electron microscope. Elemental analysis of the samples is done by EDAX EOL Model JED – 2300 make to determine the presence and percentage of bismuth, yttrium, zinc and oxygen ions. JASCO-FTIR4100/Japan is used to take FTIR studies. The UV-Visible spectra for the samples were taken using JASCO UV-Vis-NIR spectrophotometer (Model V-570) in the wavelength range 200 to 1200 nm. The photoluminescence spectrum was obtained by using FLUOROLOG, HORIBA YVON spectrophotometer.

Results and Discussion

3.1 FTIR

Figure 1 shows the FTIR spectra of pure yttrium oxide and bismuth and zinc co-doped yttrium oxide samples of three different dopant concentration prepared by sol-gel method. It was observed from Fig. 1 that the bands centred around 600 cm^{-1} is attributed to Y-O stretching mode of Y_2O_3 structure[20]. The absorption band of O-H stretching vibrations appears around 3400-3500 cm^{-1} and 1650 cm^{-1} of absorbed water which gets broad and sharp with doping concentration and it clearly shows the distortion of crystal structure and change in bond length with dopant concentration. The bands around 1020 cm^{-1} are corresponding to Zn-O stretching and deformation vibration which also increases with doping concentration. The metal-oxygen frequencies observed for the respective metal oxides are in accordance with literature values[21,22]. Parthasarathi and Thilagavathi[23] reported similar FTIR spectra observed for zinc oxide nanoparticles in their investigation. The band around 1300 cm^{-1} is attributed due to hydroxyl group bending. Around 900 cm^{-1}, Bi-O stretching vibrations has been observed for all samples.

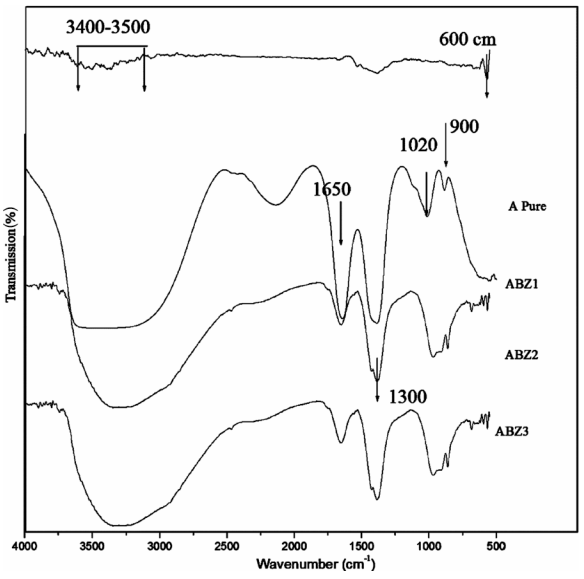

Fig. 1 – FTIR spectra of pure yttrium oxide and bismuth and zinc co-doped yttrium oxide samples prepared by sol-gel method

3.2 Structural studies

Structural analyses of samples were done by XRD and SEM.

3.2.1 XRD

XRD pattern of pure yttrium oxide and bismuth and zinc codoped yttrium oxide prepared by sol-gel method of three different dopant concentrations is shown in Fig. 2.

From Fig. 2 it is observed that the codoped samples turn out to be amorphous[24] where pure sample is found to have broad hump with emerging diffraction peaks exhibiting amorphous nature.

3.2.2 SEM

Figure 3 (a-d) shows the SEM images of pure yttrium oxide and bismuth and zinc co-doped yttrium oxide samples of three different dopant concentration

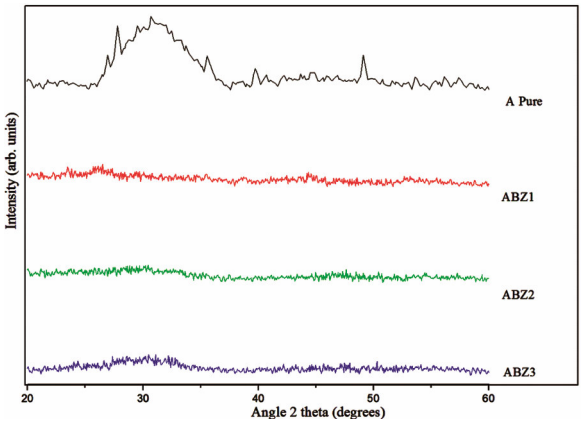

Fig. 2 – XRD of pure yttrium oxide and bismuth and zinc co-doped yttrium oxide samples prepared by sol-gel method

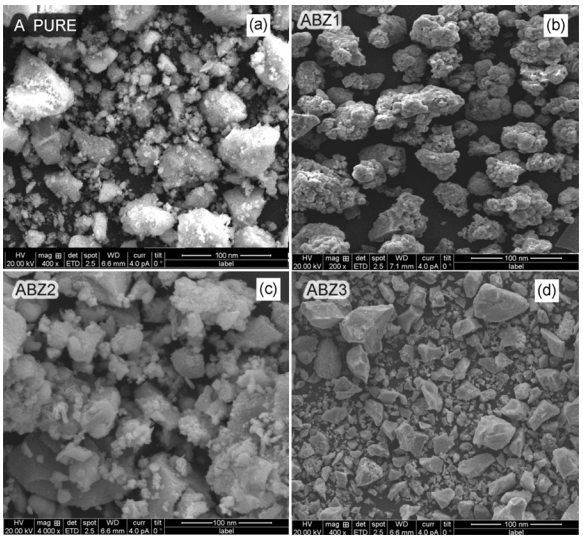

Fig. 3 – SEM images of (a) pure yttrium oxide and (b-d) bismuth and zinc doped yttrium oxide samples of three different dopant concentration prepared by sol-gel method

prepared by sol-gel method. Pure yttrium oxide sample show the cumulative nature of secondary particles which are made up of agglomeration of many primary particles. The obtained particles do not have a uniform shape and size as obtained from SEM micrographs. The Y_2O_3 particles exhibit agglomeration because of the dipole interaction[25]. SEM images of zinc and bismuth co-doped yttrium oxide samples show growth of hexagonal like structure which is found to improve with dopant concentration with the mean size of around 30±5 nm. It is observed from SEM images that the co-doped sample of lower doping concentration shows agglomeration of particles with the presence of hexagonal morphology and the SEM analysis of co-doped samples of higher doping concentration show triangular morphology along with hexagonal morphology due to the presence of bismuth[26,27].

Since Bi is incorporated as Bi_2O_3 and Zn as ZnO, the concentration of Bi in the resulting material is about two or three times higher than that of Zn. This has important consequences on the overall structure and properties[24]. Hence, triangular morphology of bismuth is predominant in the resultant morphology compared with zinc.

3.2.3 EDAX of bismuth and zinc codoped yttrium oxide

From Fig. 4 of EDAX spectrum of bismuth and zinc co-doped yttrium oxide samples prepared by sol-gel method by using ammonium hydroxide as precipitating agent of three dopant concentration, the presence of the characteristic and distinct line of yttrium (L), bismuth (L), zinc (K) and oxygen (K) have been identified. Zinc percentage is found to be very less in the samples and it was found that bismuth's concentration is more and dominant in the sample compared with zinc as identified from SEM already. It has been observed that the weight percentage of bismuth varies between 4 and 5 and zinc varies between 0.25 and 1 for the samples.

It can be seen that, in the samples, the real dopant concentration is higher than the calculated value, thus illustrating that the precipitation of dopant and yttrium is achieved with variable rates. The fact that the difference between the determined and experimental values does not show a monotonous evolution trend illustrates the complexity of the precipitation process. The formation of sample is influenced by both the solubility of dopant and yttrium precursor and the local precipitation parameters like the precipitating agent[28].

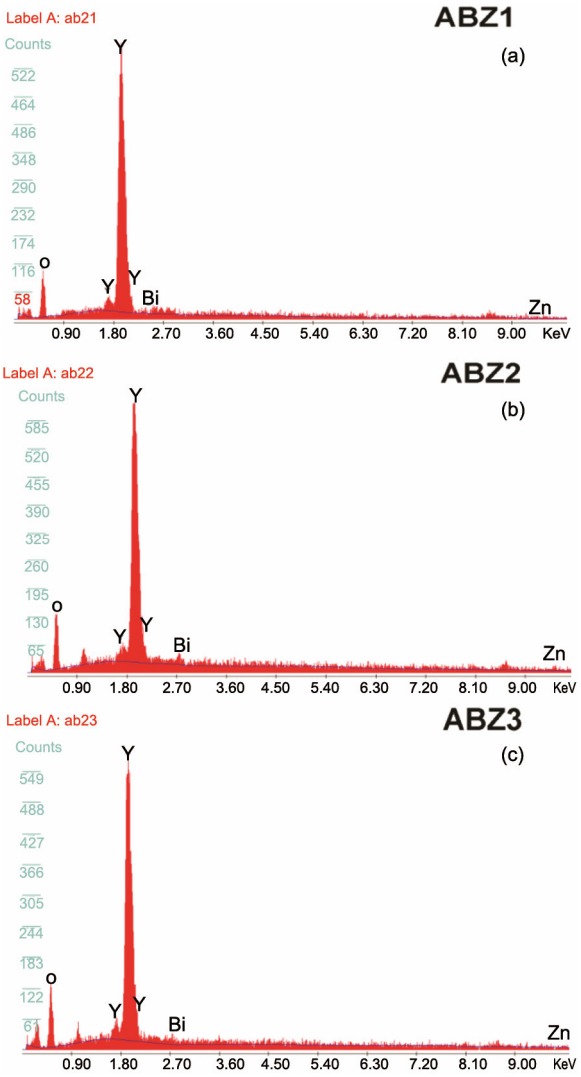

Fig. 4 – EDAX spectrum of elemental analysis of the bismuth and zinc co-doped yttrium oxide samples prepared by sol-gel method

3.3 Optical studies

Optical studies for the analysis of samples were done by UV visible absorption and PL studies.

3.3.1 UV visible absorption studies

UV visible absorbance spectrum of pure yttrium oxide and bismuth and zinc co-doped yttrium oxide prepared by sol-gel method by using ammonium hydroxide as precipitating agent of three different dopant concentration is shown in Fig. 5.

It has been observed from Fig. 5 of UV visible absorption spectrum of pure yttrium oxide and bismuth and zinc co-doped yttrium oxide samples prepared by sol-gel method by using ammonium hydroxide as precipitating agent of three different dopant concentration that pure sample shows absorption around 250 nm which is due to the

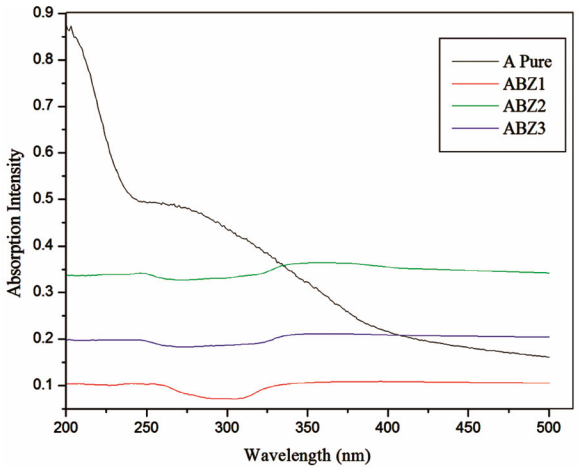

Fig. 5 –UV visible absorption of pure yttrium oxide and bismuth and zinc co-doped yttrium oxide samples prepared by sol-gel method

Table 1 – Band gap energy estimated from UV visible absorption studies of pure yttrium oxide and bismuth and zinc codoped yttrium oxide samples

Sample Name	Band gap energy (eV)
A Pure	5.17
ABZ1	4.63
ABZ2	4.44
ABZ3	4.01

absorption of yttrium oxide[29]. And for the codoped samples it has been observed that absorption occurs in UV wavelength around 325 nm due to yttrium oxide. This shift in absorption between the codoped and the undoped samples is due to quantum size effect, representing a change in band gap along with exciton features, resulting in a more discrete energy spectrum of the individual nanoparticles[30]. The effect of the quantum confinement on impurity depends upon the size of the host crystal[31]. As the size of the host crystal decreases, the degree of confinement and its effect increases[32].

Other than the peak around 325 nm, the samples are found to be completely transparent over the visible region. With doping concentration, initially the absorption increases, then the absorption intensity decreases, this shows the distortion in the crystal structure with the increase in concentration of dopants of different ionic size. Band gap energy estimated for the samples based on UV visible absorption studies[33] is given in Table 1. This result reveals that bismuth and zinc co-doped yttrium oxide samples has a weak absorption for light in the wavelength range of 300-340 nm.

It has been observed from Table 1 of band gap energy estimated from UV visible absorption studies of pure yttrium oxide and bismuth and zinc co-doped yttrium oxide samples that with doping band gap energy decreases due to the disorder introduced in the system by two different dopants of different ionic radii with respect to yttrium and of different valency. It has also been observed that the band gap energy decrease with doping concentration. It is due to the formation of impurity band and trapping of bismuth atoms, which leads to the generation of the defect states within the forbidden band[34]. Impurity band formation is an obvious consequence of increased doping concentration[35] and the trapping of the dopant atoms at the grain boundary leads to the introduction of the defect states within the forbidden band. With increasing dopant concentration, density of this dopant induced defect states increases, leading to the observed decrease of band gap or red shift. Actually, trapping of impurities and the introduction of defect states within the forbidden band gap region is intimately related to the disorder introduced in the system by doping. It is quite evident that more disorder should be introduced in the system with increasing dopant concentration as ionic radius of bismuth is slightly greater than yttrium. Hence, band gap energy decreases with dopant concentration.

From the estimated band gap energy of pure yttrium oxide and bismuth and zinc co-doped yttrium oxide samples it has been observed that there is distortion created in the yttrium oxide lattice due to the presence of the two different dopants. It was also observed that band gap energy decreases with dopant and mostly with doping concentration.

3.3.2 PL studies

The study of the photoluminescence properties is interesting because it can provide valuable information on the quality, purity and the structural properties of the material.

Photoluminescence spectrum of bismuth and zinc co-doped yttrium oxide samples prepared by sol gel method by using ammonium hydroxide as precipitating agent of three different dopant concentrations at excitation wavelength of 340 nm is shown in Fig. 6.

It has been observed from Fig. 6 of PL emission of bismuth and zinc co-doped yttrium oxide sample prepared by sol-gel method by using ammonium hydroxide as precipitating agent of three different

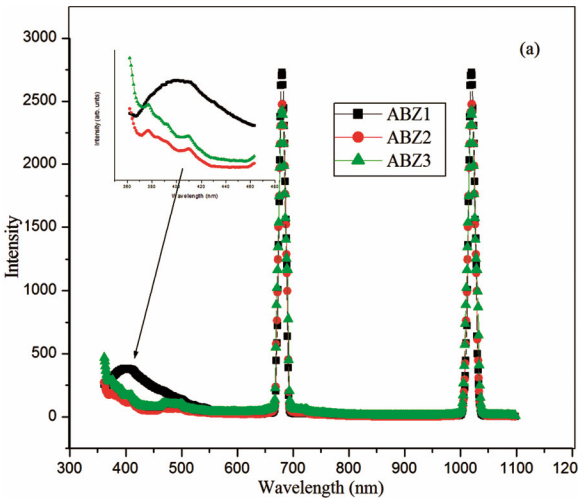

Fig. 6 – PL emission of bismuth and zinc co-doped yttrium oxide samples prepared by sol-gel method

dopant concentration has three characteristic peaks around 401 nm, 680 nm and 1020 nm. The PL peak around 401 nm corresponds to the band edge emission of zinc, which should be attributed to the recombination of excitons[36]. PL peak at 680 nm is commonly observed in bismuth doped glasses under green excitation[37]. The original peak is at 700 nm and hence the shift in peak to lower wavelength side may be due to the presence of zinc dopant of different ionic size. The emission centre in NIR region around 1020 nm is not clearly understood till now. Some researchers have reported the NIR emission due to Bi+ and some are reported as Bi5+[38]. The metallic bismuth (Bi0) NPs also causes NIR emission and has been demonstrated by various researchers[38]. PL studies show the dominance of bismuth in the samples. The result is justified by the EDAX and SEM results too. It was also observed that the PL emission intensity initially decreases then increases with doping concentration with maximum intensity at lower dopant concentration, which may be attributed due to the different dopants of different ionic size.

4 Conclusions

In this paper, structural, morphological, elemental and optical properties of pure yttium oxide and bismuth and zinc co-doped yttrium oxide samples prepared by sol-gel, method of three different dopant concentration are analysed. Presence of functional group is identified by FTIR studies. XRD analysis shows that the codoped samples are amorphous in nature. Elemental composition of the samples are

given by EDAX studies which shows that concentration of bismuth is more than zinc and the surface morphology is studied by SEM. UV visible absorption studies of pure samples show absorption due to yttrium oxide and the bismuth and zinc co-doped samples shows red shift due to dopants. From the estimated band gap energy it has been observed that band gap energy decreases with doping and dopant concentration. Bismuth and zinc co-doped yttrium oxide samples prepared by sol-gel method shows emission in violet region (401 nm) due to zinc dopant and red and NIR region (680 nm and 1020 nm) due to the bismuth dopant, which has 6 times more PL energy than due to zinc dopant. Hence, it has been concluded that yttrium oxide codoped with bismuth and zinc is a new material which can effectively work as an efficient and cheap red phosphor.

References

1 Nikl M, Novoselov A, Mihoková E, Polák K, Dusek M, McClune B, Yoshikawa A & Fukuda T, *J Phys Cond Matter*, 17 (2005) 3367.
2 Novoselov A, Yoshikawa A, Nikl M, Solovieva N & Fukuda T, *Cryst Res Technol*, 40 (2005) 419.
3 Van de Gaats A V & Blasse G, *Chem Phys Lett*, 243 (1995) 559.
4 Qiang S, Barthou C, Denis J P, Pelle F & Blanzat B, *J Lumin*, 28 (1983) 1.
5 Chi L, Liu R & Lee B, *J Electrochem Soc*, 152 (2005) 93.
6 Singh R P, Gupta K, Pandey A & Pandey A, *World J Nano Eng*, 2 (2012) 13.
7 Lopez-Luke T, De la Rosa E, Villalobos I C, Rodriguez R, Ángles-Chávez C, Salas P, Wheeler DA & Zhang J, *J Lumin*, 145 (2014) 292.
8 Dey R, Pandey A & Rai V K, *Sens Actuat B: Chem*, 190 (2014) 512.
9 Back M, Trave E, Marin R, Mazzucco N, Cristofori D & Riello P, *J Phys Chem C*, 118 (2014) 30071.
10 Pandey A, Dey R & Rai V K, *J Phys Chem Biol*, 2013 (2013).
11 Som S & Sharma S, *J Phys D: Appl Phys*, 45 (2012) 415102.
12 Yadav R, Verma R & Rai S, *J Phys D: Appl Phys*, 46 (2103) 275101.
13 Singh V, Haritha P, Venkatramu V & Kim S, *Spectrochim Acta Part A: Molecul Biomolecul Spectros*, 126 (2014) 306.
14 Suresh K, Shaik N P, Rao N V P & Murthy K V R, *Int J Nanomater Biostruct*, 4 (2014) 41.
15 Kottaisamy M & Nakanishi Y 2006, Low voltage cathodoluminescence of Zn co-doped RGB phosphors for Field Emission Displays (FEDs) applications, *Proc of ASID*, 06, 8-12 Oct, New Delhi.
16 Stanton I N, Belley M D, Nguyen G, Rodrigues A L I, Y, Kirsch D G, Yoshizumi T T & Therien M J, *Nanoscale*, 6 (2014) 5284.
17 Lojpur V, Nikolić M, Mančić L, Milošević O & Dramićanin M, *Opt Mater*, 35 (2012) 38.
18 Mishra K, Giri N K & Rai S B, *Appl Phys B: Lasers Opt*, 103 (2011) 863.
19 Subramanian R, Shankar P, Kavithaa S, Ramakrishnan S S, Angelo P C & Venkataraman H, *Mater Lett*, 48 (2001) 342.
20 Shen X & Zhai Y, *Rare Metals*, 30 (2011) 33.
21 Rao CNR, *Chemical Applications of Infrared spectroscopy* (Academic Press, New York, London), 1963.
22 Markova-Deneva I, *J Univ Chem Technol Metall*, 45 (2010) 351.
23 Parthasarathi V & Thilagavathi G, *Int J Pharm Pharm Sci*, 392 (2011).
24 Pal I, Agarwal A, Sanghi S & Aggarwal M, *Indian J Pure Appl Phys*, 51 (2013) 18.
25 Faisal M & Khasim S, *Bull Korean Chem Soc*, 34 (2013) 99.
26 Fu R, Xu S, Lu Y N & Zhu J J, *Cryst Growth Des*, 5 (2005) 1379.
27 Hwanga G H, Hana W K, Kima S J, Honga, S J, Parkb J S, Parka, H J & Kanga S G , *J Ceram Proc Res*, 10 (2009) 190.
28 Muresan L, Popovici E & Indrea E, *J Optoelectron Adv Mater*, 13 (2011) 183.
29 Zhang S & Xiao R, *J Appl Phys*, 83, (1998) 3842.
30 Viswanath R, Naik H S B, Somalanaik Y K G, Neelanjeneallu P K P, Harish K N & Prabhakara M C, *J Nanotechnol*, 2014 (2014).
31 Beecroft L L & Ober C K, *Chem Mater*, 9 (1997) 1302.
32 Kumar S, Verma, N & Singla M, *Chalcogenide Lett*, 8 (2011)561.
33 Dharma J, Pisal A & Shelton C, *Simple method of measuring the band gap energy value of TiO2 in the powder form using a UV/Vis/NIR spectrometer*, Application Note Shelton, CT- PerkinElmer (2009).
34 Karmakar R, Neogi S, Banerjee A & Bandyopadhyay S, *Appl Surf Sci*, 263 (2012) 671.
35 Pankove J I, *Optical processes in semiconductors*, Courier Corporation, (2012).
36 Vanheusden K, Warren W, Seager C, Tallant D, Voigt J & Gnade B, *J Appl Phys*, 79 (1996) 7983.
37 Denker B I, Galagan B I, Osiko V V, Shulman I L, Sverchkov S E & Dianov E M, *Appl Phys B*, 98 (2010) 455.
38 Singh S P & Karmakar B, *Mater Chem Phys*, 119 (2010) 355.